Modeling contrast perfusion and adsorption phenomena in the human left ventricle

Evandro Dias Gaio[1][0000−0003−4407−985X], Bernardo Martins Rocha[1][0000−0002−0508−8959], and Rodrigo Weber dos Santos[1][0000−0002−0633−1391]

Graduate Program in Computational Modeling.
Universidade Federal de Juiz de Fora, Juiz de Fora, Minas Gerais, Brazil

Abstract. This work presents a mathematical model to describe perfusion dynamics in cardiac tissue. The new model extends a previous one and can reproduce clinical exams of contrast-enhanced cardiac magnetic resonance imaging (MRI) of the left ventricle obtained from patients with cardiovascular diseases, such as myocardial infarct. The model treats the extra- and intravascular domains as different porous media where Darcy's law is adopted. Reaction-diffusion-advection equations are used to capture the dynamics of contrast agents that are typically used in MRI perfusion exams. The identification of the myocardial infarct region is modeled via adsorption of the contrast agent on the extracellular matrix. Different scenarios were simulated and compared with clinical images: normal perfusion, endocardial ischemia due to stenosis, and myocardial infarct. Altogether, the results obtained suggest that the models can support the process of non-invasive cardiac perfusion quantification.

Keywords: Myocardial perfusion · Adsorption · Ischemia · Left Ventricle Dynamics.

1 Introduction

Cardiovascular diseases are one of the major causes of death worldwide [14]. These conditions include coronary atherosclerosis, aortic valve regurgitation, and left ventricle hypertrophy, which affect the myocardium perfusion (MP), reduce oxygen delivery (ischemia), cause tissue damage, and lead to infarct. Contrast-enhanced Magnetic Resonance Imaging (MRI) is an exam that seeks to characterize myocardial perfusion and detect scars or infarct regions by conducting a contrasting agent (CA) to the patient. On the images generated by a specific protocol, the CA assumes a specific contrast on poorly perfused regions, which allows its identification. The most used protocol is the Late Gadolinium Enhancement (LGE), a technique used in heart MRI for cardiac tissue characterization. Particularly, LGE allows the assessment of myocardial scar formation and regional myocardial fibrosis when the gadolinium, the CA, is perfused for about 600 seconds and is adsorbed in areas of excess of extracellular matrix.

ICCS Camera Ready Version 2022
To cite this paper please use the final published version:
DOI: 10.1007/978-3-031-08754-7_52

Blood-tissue exchange investigation is a topic of long-standing interest to physiologists and was first modeled mathematically as a set of reaction-diffusion-advection equations by [4]. More recently, [16] has proposed a framework for the simulation of cardiac perfusion using Darcy's law within the idea of multi-compartment to represent the different blood vessel's spatial scale. In the field of medical image analysis, [7] has proposed to quantify the behavior of contrast agents in MR perfusion imaging. This work has used a simplified model of contrast agent transport and provided interesting insights on the design and selection of the appropriate CA for specific imaging protocol and post-processing method. Finally, [2, 1] proposed similar tools that also uses mathematical models based on PDEs (Partial Differential Equations) and images, in this case, from contrast-enhanced MRI exams. In particular, the previous work presented in [1] evaluated the CA dynamics for three different scenarios: healthy, ischemic, and infarct in a 2D mesh slice from an MRI exam and performed a comparison with experimental data for the LGE protocol.

In this work, we present an extended model for describing the perfusion of the contrasting agent in cardiac tissue based on porous media flow, which is suitable for 3D geometries and patient-specific models generated through image segmentation from MRI [1, 18]. The mathematical model uses Darcy's law for the extra- and intravascular regions and is coupled to a reaction-diffusion-advection equation for the CA dynamics. Through a series of numerical experiments, we show that the model can correctly reproduce clinical exams via computer simulations during normal perfusion and in the presence of ischemia or myocardial infarct. In addition, we also present the pipeline used for generating patient-specific finite element meshes appropriate for the simulations of the perfusion model. This study has a potential high impact since it combines information from two different exams: Fractional Flow Reserve (FFR) Measurement of the heart coronaries from CT and heart perfusion and topology from MRI scan [3, 19].

2 Methods

2.1 Mathematical Modeling

There are many different ways to represent and deal with circulatory models in the literature [4, 16, 7]. In this work, the perfusion is modeled through a reaction-diffusion-advection equation in porous media. Even knowing that blood vessels have non-trivial topological features, a simplified representation of the domain can provide useful insights in many aspects and can be used to reproduce clinical exams of contrast-enhanced cardiac MRI of the whole heart.

A porous medium is a solid filled and connected by voids, where the ratio between the volume of void space and the total volume is called porosity, which is given by:

$$\phi = \frac{V_p}{V_t}, \tag{1}$$

where V_p is the volume of the void (or porous) space and V_t is the total volume.

ICCS Camera Ready Version 2022
To cite this paper please use the final published version:
DOI: 10.1007/978-3-031-08754-7_52

Porous Media Flow in the Intravascular Domain Darcy's law is used to describe flow in porous media, and can be expressed through the following equations for an incompressible fluid low:

$$\mathbf{v} = -\mathbf{K}\nabla p, \quad \text{in } \Omega, \tag{2}$$

$$\nabla \cdot \mathbf{v} = \alpha, \quad \text{in } \Omega, \tag{3}$$

where $\mathbf{v}$ is the velocity, p is the pressure, $\mathbf{K}$ is the permeability tensor, α is a source term, and Ω is the left ventricular domain (LV).

The tensor $\mathbf{K}$ must represent the anisotropy and heterogeneity of the intravascular domain due to the fibers presents in cardiac microstructure, as described in [1, 7]. The heterogeneity is first represented by a transmural gradient of permeability (w) by solving the Laplace equation ($\nabla^2 w = 0$), using Dirichlet boundary condition at the epicardial ($w = 1$) and endocardial ($w = 0$) boundaries, respectively. The permeability tensor including anisotropy and heterogeneity can be described as:

$$\mathbf{K} = K_t\mathbf{I} + (K_l - K_t)\mathbf{f} \otimes \mathbf{f} \tag{4}$$

where $\mathbf{f}$ is the unit vector that represents the preferential direction of permeability which follows the myocardial fiber orientation, K_l is the permeability value along the fiber direction $\mathbf{f}$, and K_t is the permeability in the transversal direction. The values of these permeabilities are given by:

$$K_l = K_1(1-w) + 2K_1 w, \quad K_t = K_2(1-w) + 2K_2 w \tag{5}$$

where K_1 and K_2 are the permeabilities in outer boundary, with K_1 approximately 10.8 times higher than K_2 [7].

Contrast Agent Dynamics in the Intra- and Extravascular Domains Contrast agent dynamics can be described by a system of diffusion-advection equations in a bidomain composed of the intra- and extravascular regions. The intravascular represents the combination of arteries and capillaries, whereas the extravascular represents the interstitial space, and possibly a region with fibrosis, when it is considered. The equations governing the dynamics of the concentrations of CA in the intra- and extravascular regions, denoted by C_i and C_e, respectively, are given by:

$$\frac{\partial(\phi C_i)}{\partial t} + \nabla \cdot (\mathbf{v}C_i) - \phi\nabla \cdot (\mathbf{D}_i \nabla C_i) + f = 0, \quad \text{in } \Omega_i, \tag{6}$$

$$\frac{\partial((1-\phi)\lambda C_e)}{\partial t} - (1-\phi)\lambda\nabla \cdot (\mathbf{D}_e \nabla C_e) - f + (1-\phi)\lambda k_e C_e + g = 0, \text{in } \Omega_e, \tag{7}$$

where $\mathbf{D}_i$ and $\mathbf{D}_e$ are diffusion tensors for the intra- and extravascular regions, respectively, f represents the communication between the domains which is given by:

$$f = \begin{cases} P(C_i - C_e), & \text{if} \quad C_i > C_e, \\ 0, & \text{otherwise}, \end{cases} \tag{8}$$

ICCS Camera Ready Version 2022
To cite this paper please use the final published version:
DOI: 10.1007/978-3-031-08754-7_52

where P is the endothelial permeability. The term $(1-\phi)\lambda k_e C_e$ models the flow from the interstitial space to the venous system, and λ represents the fraction of the extravascular domain that is occupied by the interstitial space.

Contrast Agent Adsorption In addition, another equation and variable is needed to capture how the CA is trapped in the excess of extracellular matrix, which is the case of fibrosis or scar. This phenomenon, fluid (CA) attaching to a solid phase (extracellular matrix), is called adsorption, and is modeled by:

$$\frac{\partial((1-\phi)\lambda\lambda_f C_f)}{\partial t} + (1-\phi)\lambda\lambda_f k_f C_f - g = 0, \quad \text{em} \quad \Omega_f, \tag{9}$$

where C_f is the concentration of CA in the fibrosis network domain Ω_f, g is a exchange term between the fibrotic and extravascular domains, and the $k_f C_f$ term describes the flow from the fibrotic network to the venous system. The exchange term g is given by:

$$g = (1-\phi)\lambda\lambda_f k_{ef} C_e, \tag{10}$$

where k_{ef} is the rate at which the contrast moves from the interstitium to the fibrosis, and λ_f is the fraction of the interstitium occupied by the region with fibrosis.

Recirculation of the Contrast Agent During MRI or CT scan, the cyclic behavior of the CA is captured. Part of the CA is retained by the kidneys for elimination, but a certain amount, after a while, returns by the blood flow itself and is infused into the cardiac tissue again by the coronary arteries, i.e., the intravascular domain.

To represent this behavior of the CA, a reaction-diffusion-advection equation in a one dimensional domain (of size L) is used. The total amount of CA in the intravascular domain of the myocardium is imposed as an inflow into the 1D domain. The parameters of the equation were defined so that the time and the amount of flux at the output of the 1D domain represent the physiological behavior. Therefore, the amount of flow at the exit of the 1D domain is imposed as a recirculation parameter $X(\mathbf{x}, t)$ for the boundary condition of the CA flow in the intravascular domain.

The recirculation is therefore described by the following equation:

$$\frac{\partial C_{out}}{\partial t} + \nabla \cdot v_{out} C_{out} - \nabla \cdot (D_{out} \nabla C_{out}) + k C_{out} = 0, \quad \text{in} \quad [0, L], \tag{11}$$

where v_{out} and D_{out} represents the velocity or convection term and the diffusion respectively of this re-circulatory system, discussed numerically in [1]. This equation is subject to the following conditions:

$$C(0,t) = \frac{\int_{\Omega_i} C_i \, d\Omega_i}{|\Omega_i|}, \quad X(\mathbf{x}, t) = C(L, t). \tag{12}$$

ICCS Camera Ready Version 2022
To cite this paper please use the final published version:
DOI: 10.1007/978-3-031-08754-7_52

Initial and boundary conditions The boundary conditions for the Darcy equation (2) are of the Dirichlet type, and are given by:

$$p = p_o, \quad \text{on} \quad \Gamma_{epi}, \tag{13}$$
$$p = p_i, \quad \text{on} \quad \Gamma_{endo}. \tag{14}$$

For CA dynamics subsystem, a convective and diffusive flow of CA inflow into the intravascular domain through the epicardium is imposed, controlled by a transient Gaussian function, which is given by:

$$\mathbf{v}C_i - \mathbf{D}_i \nabla C_i = \mathbf{v}Q(t), \quad \text{on} \quad \Gamma_{epi}, \tag{15}$$

with $Q(t)$ given by

$$Q(t) = \frac{1}{\sigma\sqrt{2\pi}} e^{-\frac{1}{2}\left(\frac{t - t_{peak}}{\sigma}\right)} + X(t, \vec{x}), \tag{16}$$

where σ^2 reflects the variance of the CA infusion, t_{peak} is the Gaussian mean which is the peak value of the function, and $X(t, \vec{x})$ is the additional term generated by CA recirculation due to the cyclic behavior of the blood system.

No-flux boundary conditions are used for the other boundaries, as follows:

$$\mathbf{D}_i \nabla C_i \cdot \mathbf{n} = 0 \quad \text{on} \quad \Gamma_{endo}, \tag{17}$$
$$\mathbf{D}_e \nabla C_e \cdot \mathbf{n} = 0 \quad \text{on} \quad \Gamma_{endo}, \tag{18}$$
$$\mathbf{D}_e \nabla C_e \cdot \mathbf{n} = 0 \quad \text{on} \quad \Gamma_{epi}. \tag{19}$$

2.2 Left Ventricular Geometry Models

In this work, two geometries for representing the left ventricle were used. The first one is the simplified representation of the LV as a family of truncated ellipsoids. Parametric equations were used to allow better geometric control, ideal for defining contours (endocardium and epicardium) and well-defined positioning of subdomains (fibrosis), as shown in Figure 1A.

There are also heterogeneity and anisotropy in the properties of the models. Heterogeneity occurs since the subendocardial permeability is, on average, twice as high as the subepicardial permeability. Moreover, anisotropy is due to the fiber direction being the preferred direction of the microvascular system, that is, the preferential direction for perfusion. These characteristics are translated to the permeability tensor $\mathbf{K}$.

To generate the fibers, the *Laplace-Dirichlet Rule-Based (LDRB)* algorithm [5] was used. The algorithm requires as inputs the helical angles for the fibers on endocardium and epicardium surfaces, marked subdomains (left ventricle (LV) and right ventricle (RV)), and contours (base, epicardium, and endocardium). It generates vectors describing the fiber direction, sheet direction, and normal direction as outputs. An illustrative example of the result of the LDRB algorithm for generating the fiber orientation field is shown in Figure 1B.

ICCS Camera Ready Version 2022
To cite this paper please use the final published version:
DOI: 10.1007/978-3-031-08754-7_52

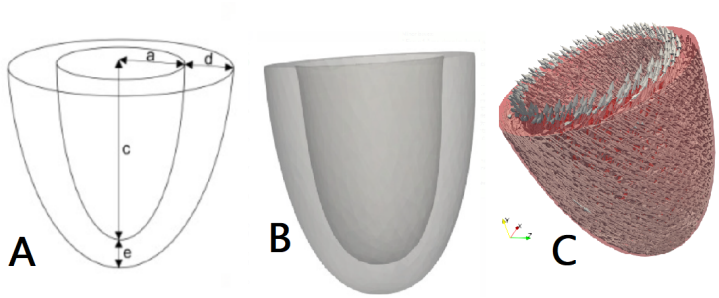

Fig. 1. **(A)** Parametric representation of the LV geometry: d,e = 1.0 cm, c = 6.0 cm, a = 2.0 cm. **(B)** Finite element mesh. **(C)** Fiber orientation field generated by the LDRB algorithm on a simplified LV mesh.

The study considers a patient-specific geometric model. For this study case, the following pipeline was considered. First, image segmentation of the LV from MRI is performed as described in [8]. This method produces a finite element mesh with a high spatial resolution. Second, scar regions are marked, which is required for the numerical studies carried out in this work (see Figure 2B). The next step consists in generating a coarser mesh since the initial one is highly refined and would result in a huge computational effort for numerical simulation. Mesh processing techniques were used to get a coarser mesh keeping the same topology and reducing by about 90% the number of elements (see Figure 2C). This step was carried out using the `meshtool` software [17]. Finally, the geometrical model is complemented with fiber and sheet orientation fields (see Figure 2A and C).

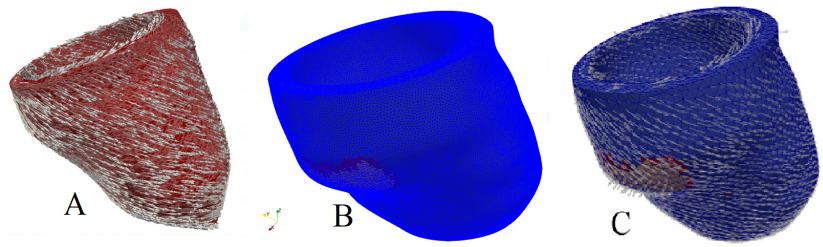

Fig. 2. Patient-specific meshes. **(A)** Fibers orientation, used in perfusion permeability tensor. **(B)** Mesh with marked scars and huge number of elements. **(C)** Used mesh for numerical simulations.

2.3 Numerical methods

The differential equations presented in the mathematical modeling part were solved using the finite element method. In comparison with [1], where the reduced

ICCS Camera Ready Version 2022
To cite this paper please use the final published version:
DOI: 10.1007/978-3-031-08754-7_52

Darcy approximation was used, in this work, Darcy's problem is solved by using a mixed formulation [11] in terms of both pressure and velocity fields. For this goal, two discrete function spaces are needed to form a mixed function space and a stable choice of finite element spaces is the $\mathbf{H}(div)$ Brezzi-Douglas-Marini elements of polynomial order 1 and the discontinuous Lagrange elements $\mathbf{L}^2$ of order 0. In addition to ensuring the consistency of mass conservation at the macro scale level, this method is more suitable to impose flux as a boundary condition besides only pressure. More details about the numerical formulation may be found in [13].

The transient CA transport equations (6),(7), and (11) were discretized with the Crank-Nicolson scheme, which is unconditionally stable and second-order accurate. The transport problem was discretized in space with the finite element method using first-order continuous Lagrange elements. Due to the presence of convective terms in the intravascular Eq. (6) and the recirculation Eq. (11), stabilization terms from the *Streamline upwind Petrov–Galerkin (SUPG)* method [6] were added for these equations.

3 Results and Discussion

In this section, we first present some numerical results with a simplified 3D model based on an idealized ellipsoid for comparisons and validation. Then, after a proper calibration of the mathematical model [1], we perform simulations on a patient-specific model constructed after image segmentation and processing.

All computer simulations were performed in a personal computer equipped with an 8th generation i7 3200GHz processor and 16 GB of memory. The execution time to simulate a mesh with $47,662$ tetrahedral elements and $10,232$ nodes was around 3 hours.

3.1 Simplified LV Model Study

The parameters used for the simulations are presented in Table 1 and were based on those reported in [1]. The ellipsoid simulation involves three different scenarios. The first is the Normal scenario which considers a healthy ventricle, represented by a uniform gradient pressure from epicardium (2kPa) to endocardium (0kPa). The second scenario represents an Ischemic case by assuming a restriction in blood supply from the coronaries, which was modeled here by a 30% of pressure drop (1.4kPa) in a small region of the epicardium. Both Normal and Ischemic cases share the same physical tissue parameters. The third scenario represents an Infarct where a more significant pressure drop of 50% (1kPa) is considered in the same region of the ischemic case. This case has an additional small infarcted region next to the endocardium at the same side where the pressure drop is applied. It is represented by a subdomain of dead tissue, which is modeled using parameters representing the infarct (see Table 1). The main differences between Healthy, Ischemic, and Infarct cases are the addition of this

ICCS Camera Ready Version 2022
To cite this paper please use the final published version:
DOI: 10.1007/978-3-031-08754-7_52

Table 1. Parameters used for the numerical simulations.

Parameter (unity)	Healthy/Ischemic	Infarct
k_e (s^{-1})	0.007	0.002
$P(s^{-1})$	1.0	1.0
$k_f(s^{-1})$	0	0.001
$k_{ef}(s^{-1})$	0	0.01
ϕ	0.10	0.10
λ	0.25	1.0
λ_f	0	0.5
$D(mm^2s^{-1})$	0.01	0.01
σ	6.0	6.0
$t_{peak}(s)$	25	25
$v_{out}(mm.s^{-1})$	0.06	0.06
$D_{out}(mm^2s^{-1})$	0.05	0.05
$k(s^{-1})$	0.01	0.01

new subdomain and reducing the k_e parameter to represent the difficulty of flow from the interstitial space back to the venous system in a fibrotic region.

Figure 3 shows the results of the LGE simulation obtained using the simplified LV geometry for the three cases: normal, ischemic, and infarct. This exam is used to reveal dead tissue by the absorption phenomena. Therefore, as expected, the results show that only the infarct case presents CA adsorption. These scenarios reproduced characteristics usually observed by clinicians. It is important to remark here that this preliminary study using 3D left ventricular meshes conforms with the one presented in [1], where simpler 2D cases were studied.

Figures 4 and 5 shows a quantitative comparison between the 3D idealized geometry and experimental clinical data with respect to the signal intensity (SI) of the contrast agent (sum of the CA concentration) for specific regions of interest (ROI) of the first pass ($50s$) and LGE, respectively. In order to compare the CA dynamics, two ROIs were marked: one represents the injured region and the other represents a remote and healthy region. In addition, a linear relationship between the concentration of CA and its SI was considered [9]. The comparative curves between the simulated scenarios and the experimental data show that these results are in agreement with those found in the literature [10, 20] for the first pass (Figure 4), as well as for the LGE [12, 3] (Figure 5). The results are also in consonance to the results previously found by [1].

Figure 6(a) shows pressure field results of Darcy's problem for the idealized LV problem. The pressure gradient is imposed as boundary values and a smaller pressure (see Figure 6(a), right of epicardium) is used to simulate pathologies (coronary artery diseases (CAD) or ischemic heart diseases (IHD)). Panel (b) from Figure 6 presents the adsorption of CA in the ROI, which is characterized by a region with high contrast values as a result of the trapped gadolinium, revealing dead tissue.

ICCS Camera Ready Version 2022
To cite this paper please use the final published version:
DOI: 10.1007/978-3-031-08754-7_52

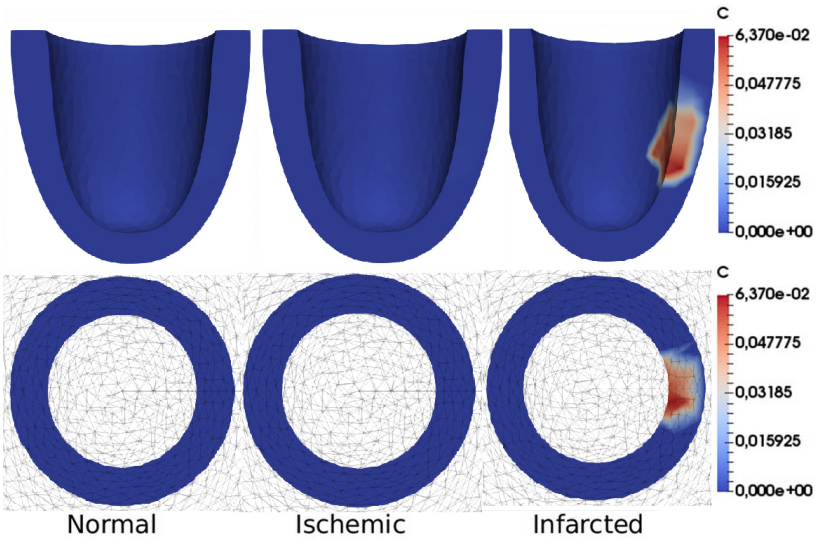

Fig. 3. Computer simulations of the LGE (600 s) for normal, ischemic, and infarcted left ventricles. After some time, the CA reveals adsorption in the infarcted region, as observed in the region with high contrast values on the right panel.

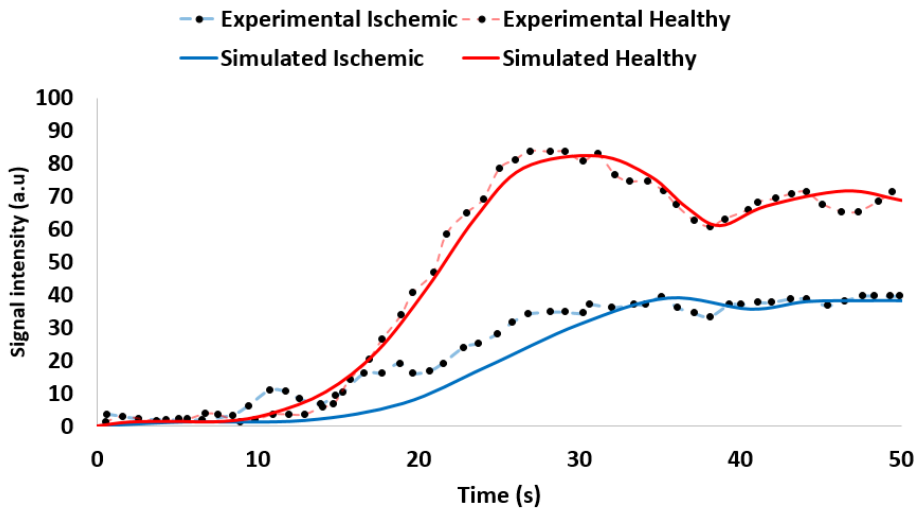

Fig. 4. First pass comparison of healthy and ischemic cases between this numerical study and experimental data reported in [10].

3.2 Patient Specific LV Study

The following study case explored a simulation using a patient-specific LV mesh. The same procedure was carried out here, but now with the difficulties of han-

ICCS Camera Ready Version 2022
To cite this paper please use the final published version:
DOI: 10.1007/978-3-031-08754-7_52

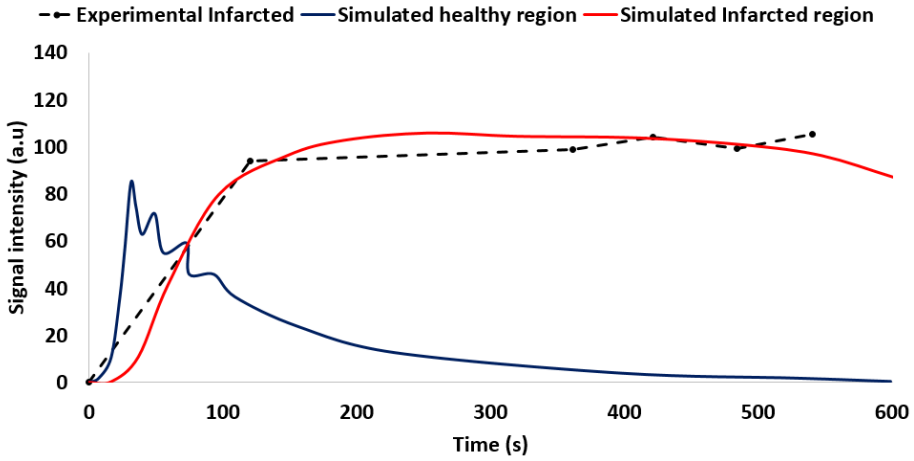

Fig. 5. Late-enhancement time evolution of CA in the fibrosis region (infarct) and a remote (healthy) one. Comparison of cases between this numerical study and clinical data from [12].

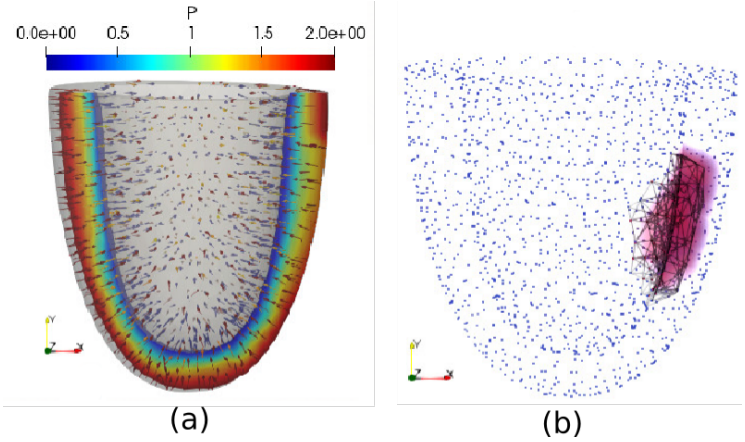

Fig. 6. Simulation results for idealized model. (a) Perfusion of CA flux induced by pressure gradient. (b) CA adsorbed at the fibrosis region (black wired) represented over the domain (dots).

dling a realistic and complex geometry. The LV mesh used for this case was processed from the geometries available at a database from Kings College London (more information is available in [15]). The parameters used were those presented in Table 1, except for $D = 0.05$, $P = 0.1$, $k_e = 0.0009$ and $\lambda = 0.75$.

Figure 7A shows the result of Darcy's problem for the patient-specific problem. The pressure gradient is imposed as boundary values and a pressure drop was used to simulate coronary artery disease. The arrows in the figure repre-

ICCS Camera Ready Version 2022
To cite this paper please use the final published version:
DOI: 10.1007/978-3-031-08754-7_52

sent Darcy's flux, which is used in the convection term of the CA. Figure 7B presents the adsorption of CA in the fibrosis region (black wired). As expected, these results are similar to the ones presented in Figure 6 for the simplified LV geometry.

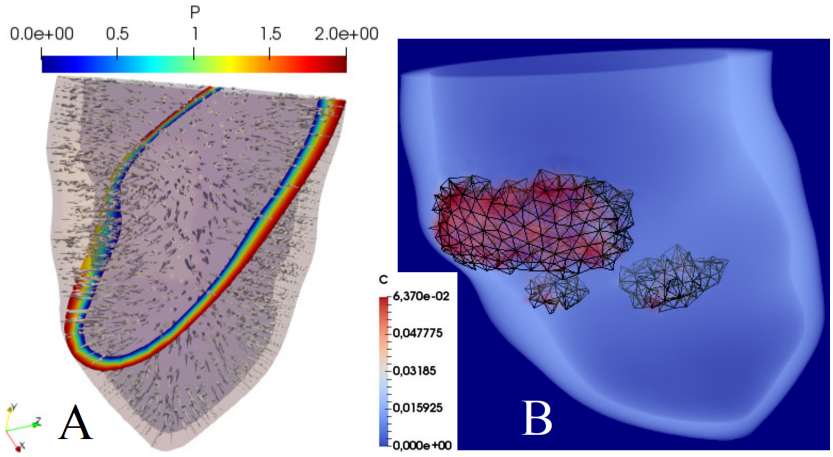

Fig. 7. Simulation results for the patient specific LV model. (a) Perfusion of CA flux induced by the pressure gradient. (b) CA adsorbed at the fibrosis region (black wired) represented over the domain.

Results for the LGE protocol are shown in Figure 8, where we observe an accumulation of trapped CA in the fibrotic region. The results agree with the literature, demonstrating the validity of this numerical study for a patient-specific case.

Figure 9 presents a comparison between the results obtained with the simplified ellipsoidal model, the patient-specific model, and clinical data. One can observe qualitative similar dynamics. In addition, we observe that the amount of trapped CA in the infarct region is higher in the patient-specific model than in the other experiments. This is expected since the infarct region of the patient was observed to be larger than the one used in the ellipsoid-based model.

4 Conclusions

The main contribution of this study was to advance the computational models of cardiac perfusion and, more specifically, to apply them in realistic scenarios, such as clinical studies involving patient-specific models. For this goal, the mathematical model presented in [1] was used since it was able to reproduce clinical data.

Numerical experiments using a simplified 3D LV model were first performed to validate the mathematical model and the numerical approach since they were

ICCS Camera Ready Version 2022
To cite this paper please use the final published version:
DOI: 10.1007/978-3-031-08754-7_52

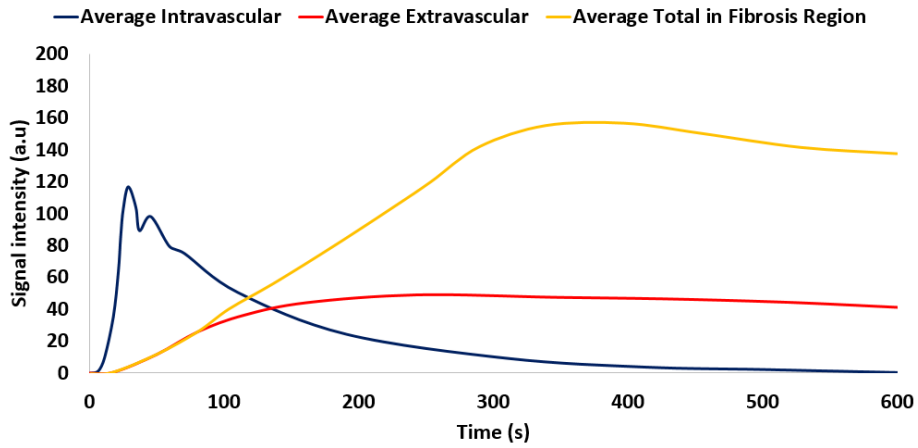

Fig. 8. Late-enhancement time evolution of CA for patient specific model with fibrosis. Blue and red line represents the intravascular and extravascular average quantity respectively in the healthy medium. The yellow line represents the average of total CA at the fibrosis domain.

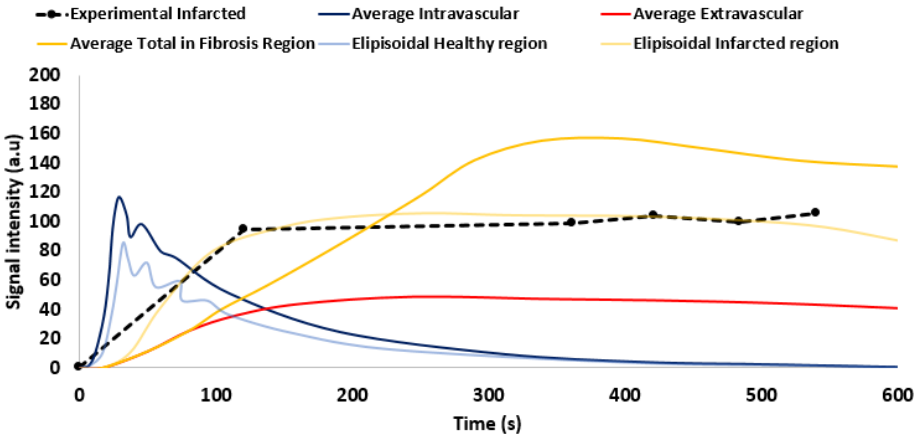

Fig. 9. Comparison of the late enhancement time evolution of CA between the simplified ellipsoidal model, the patient-specific LV model, and clinical data.

only tested in 2D cases before. The obtained results reproduced with great accuracy the clinical data. Therefore, our mathematical model and numerical methods are suitable for 3D realistic simulations of cardiac perfusion under different pathological conditions, such as ischemia and infarct.

Finally, we developed a patient-specific LV model for the description of cardiac perfusion. The precise shapes of the left ventricle and of the scar of the patient were obtained from MRI data. Distance and scars were evaluated and

ICCS Camera Ready Version 2022
To cite this paper please use the final published version:
DOI: 10.1007/978-3-031-08754-7_52

marked, and mesh operations were performed for the numerical optimization of the presented studies. The simulations of the 3D patient-specific model were performed and the results were found to be in agreement with the literature and with the available experimental data.

In the near future, we expect to extend the presented framework for the modeling of cardiac perfusion to other patients and to other cardiac diseases.

Acknowledgements This work was supported by UFJF, CAPES, CNPq (Grants 310722/2021-7, 315267/2020-8), and FAPEMIG (Grants APQ-01340-18, APQ 02489/21).

References

1. Alves, J.R., de Queiroz, R.A., Bär, M., Dos Santos, R.W.: Simulation of the perfusion of contrast agent used in cardiac magnetic resonance: A step toward non-invasive cardiac perfusion quantification. Frontiers in physiology **10**, 177 (2019)
2. Alves, J., de Queiroz, R., dos Santos, R.: Simulation of cardiac perfusion by contrast in the myocardium using a formulation of flow in porous media. Journal of Computational and Applied Mathematics **295**, 13–24 (2016)
3. Arai, A.E.: The cardiac magnetic resonance (CMR) approach to assessing myocardial viability. Journal of Nuclear Cardiology **18**(6), 1095–1102 (2011)
4. Bassingthwaighte, J., Wang, C., Chan, I.: Blood-tissue exchange via transport and transformation by capillary endothelial cells. Circulation research **65**(4), 997–1020 (1989)
5. Bayer, J.D., Blake, R.C., Plank, G., Trayanova, N.A.: A novel rule-based algorithm for assigning myocardial fiber orientation to computational heart models. Annals of biomedical engineering **40**(10), 2243–2254 (2012)
6. Brooks, A.N., Hughes, T.J.: Streamline upwind/petrov-galerkin formulations for convection dominated flows with particular emphasis on the incompressible navier-stokes equations. Computer methods in applied mechanics and engineering **32**(1-3), 199–259 (1982)
7. Cookson, A.N., Lee, J., Michler, C., Chabiniok, R., Hyde, E., Nordsletten, D., Smith, N.: A spatially-distributed computational model to quantify behaviour of contrast agents in mr perfusion imaging. Medical image analysis **18**(7), 1200–1216 (2014)
8. Costa, C.M., Neic, A., Kerfoot, E., Porter, B., Sieniewicz, B., Gould, J., Sidhu, B., Chen, Z., Plank, G., Rinaldi, C.A., et al.: Pacing in proximity to scar during cardiac resynchronization therapy increases local dispersion of repolarization and susceptibility to ventricular arrhythmogenesis. Heart rhythm **16**(10), 1475–1483 (2019)
9. Daly, C., Kwong, R.Y.: Cardiac mri for myocardial ischemia. Methodist DeBakey cardiovascular journal **9**(3), 123 (2013)
10. Daly, C., Kwong, R.Y.: Cardiac mri for myocardial ischemia. Methodist DeBakey cardiovascular journal **9**(3), 123 (2013)
11. Duran, O., Devloo, P.R., Gomes, S.M., Valentin, F.: A multiscale hybrid method for darcy's problems using mixed finite element local solvers. Computer methods in applied mechanics and engineering **354**, 213–244 (2019)

ICCS Camera Ready Version 2022
To cite this paper please use the final published version:
DOI: 10.1007/978-3-031-08754-7_52

12. Knowles, B.R., Batchelor, P.G., Parish, V., Ginks, M., Plein, S., Razavi, R., Schaeffter, T.: Pharmacokinetic modeling of delayed gadolinium enhancement in the myocardium. Magnetic Resonance in Medicine: An Official Journal of the International Society for Magnetic Resonance in Medicine **60**(6), 1524–1530 (2008)
13. Logg, A., Mardal, K.A., Wells, G.: Automated solution of differential equations by the finite element method: The FEniCS book, vol. 84. Springer Science & Business Media (2012)
14. Mehta, P.K., Wei, J., Wenger, N.K.: Ischemic heart disease in women: a focus on risk factors. Trends in cardiovascular medicine **25**(2), 140–151 (2015)
15. Mendonca, C. C.; Neic, A., et al.: A virtual cohort of twenty-four left-ventricular models of ischemic cardiomyopathy patients. King's College London Dataset (2020)
16. Michler, C., Cookson, A., Chabiniok, R., Hyde, E., Lee, J., Sinclair, M., Sochi, T., Goyal, A., Vigueras, G., Nordsletten, D., et al.: A computationally efficient framework for the simulation of cardiac perfusion using a multi-compartment darcy porous-media flow model. International journal for numerical methods in biomedical engineering **29**(2), 217–232 (2013)
17. Neic, A., Gsell, M.A., Karabelas, E., Prassl, A.J., Plank, G.: Automating image-based mesh generation and manipulation tasks in cardiac modeling workflows using meshtool. SoftwareX **11**, 100454 (2020)
18. Niederer, S.A., Aboelkassem, Y., Cantwell, C.D., Corrado, C., Coveney, S., Cherry, E.M., Delhaas, T., Fenton, F.H., Panfilov, A.V., Pathmanathan, P., Plank, G., Riabiz, M., Roney, C.H., dos Santos, R.W., Wang, L.: Creation and application of virtual patient cohorts of heart models. Philosophical Transactions of the Royal Society A: Mathematical, Physical and Engineering Sciences **378**(2173), 20190558 (2020)
19. Taylor, C.A., Fonte, T.A., Min, J.K.: Computational fluid dynamics applied to cardiac computed tomography for noninvasive quantification of fractional flow reserve: Scientific basis. Journal of the American College of Cardiology **61**(22), 2233–2241 (2013)
20. Wang, J., Xiang, B., Lin, H.y., Liu, H.y., Freed, D., Arora, R.C., Tian, G.h.: Collateral circulation formation determines the characteristic profiles of contrast-enhanced mri in the infarcted myocardium of pigs. Acta Pharmacologica Sinica **36**(4), 463–472 (2015)

ICCS Camera Ready Version 2022
To cite this paper please use the final published version:
DOI: 10.1007/978-3-031-08754-7_52